ejpmr, 2017,4(10), 436-442

SJIF Impact Factor 4.161

EUROPEAN JOURNAL OF PHARMACEUTICAL AND MEDICAL RESEARCH

www.ejpmr.com

Research Article

ISSN 2394-3211

EJPMR

TRACE LEVEL RECOGNITION OF PB^{2+} AND I^- IONS IN AQUEOUS MEDIUM USING A PYRIDO-PYRIMIDINE CHEMOSENSOR: EXPERIMENTAL AND DFT STUDIES

Samadhan R. Patil[1], Jitendra P. Nandre[1], Prashant A. Patil[2], Pritesh R. Jain[1], Suban K. Sahoo[3], Chullikkattil P. Pradeep[4], Debasis Das[5], Timothy J. Prior[6], Carl Redshaw[6], Umesh D. Patil[2], Ashok A. Patil*[1]

[1]Department of Organic Chemistry, JET'S Z.B.Patil, College, Deopur, Dhule-424 001, (M.S.) INDIA.
[2]S.S.V.P.S's L. K. Dr. P. R. Ghogrey Science College, Dhule-424 001, INDIA.
[3]Department of Applied Chemistry, S.V. National Institute Technology, Surat-395 007, Gujrat, INDIA.
[4]School of Basic Sciences, Indian Institute of Technology Mandi, Kamand-175005, Himachal Pradesh, INDIA.
[5]Department of Chemistry, The University Burdwan, Golapbag, 713104, West Bengal; INDIA.
[6]Department of Chemistry, University of Hull, Cottingham Road, Hull, HU6 7RX (UK).

***Corresponding Author: Prof. Dr. Ashok A. Patil**

Department of Organic Chemistry, JET'S Z.B.Patil, College, Deopur, Dhule-424 001, (M.S.) INDIA.

Article Received on 21/08/2017 **Article Revised on 11/09/2017** **Article Accepted on 01/10/2017**

ABSTRACT

The new chemosensor, 7-bromo-4-imino-2-(methylthio)-4*H*-pyrido[1,2-*a*]pyrimidine-3-carbonitrile (**PP-1**), which bears a pyrido-pyrimidine unit, has been synthesized and fully characterized. Whilst Pb^{2+} and I^- ions caused distinguishable changes in the absorption spectrum of **PP-1**, the other common cations and anions which were tested had no effect. The sensor **PP**-1 exhibited detection limits down to 0.21 µM and 0.1 µM for Pb^{2+} and I^- ions, respectively. HRMS analysis, ^{1}H NMR titrations and DFT calculations have been performed to elucidate the binding interaction between the sensor **PP-1** and the analytes (Pb^{2+} and I^-).

KEYWORDS: Chemosensor, Pyrido-pyrimidine, Pb^{2+}, I^-, DFT.

1. INTRODUCTION

In recent years, tremendous effort has been devoted towards the synthesis and development of chemosensors for the selective and sensitive determination of heavy and transition metal ions, particularly those which have important physiological and environmental impacts.[1-3] The emancipation of poisonous heavy metal ions into the environment is problematic. Being of non-biodegradable nature, heavy metal ions have a propensity to accumulate in organisms and enter the food chain through a variety of pathways, and as a result are a serious concern to human health.[4] Pb^{2+}, one of the most encountered toxic heavy metal ions, is widely distributed in the environment and extensively used in batteries, gasoline and pigments.[5] The 'Center for Disease Control and Prevention' have reported that ~ 250,000 young children in the USA have blood lead level more than 10 µg/dL, which is well above the acceptable limit.[6] The FDA limit for lead in drinking water is 0.015 mg/L (7.2×10^{-8} M).[7] Lead poisoning causes neurological damage, anemia, physical growth impairments, nerve disorders, kidney disorders, memory loss and reduced IQ.[8,9] At the same time, considerable research has focused on the selective recognition of anions of importance in biological, industrial and environmental processes. Amongst them, iodide, an indispensable microelement, plays an important role in several biological activities *viz.* brain functions, cell growth, neurological activities, metabolisms and thyroid functions. Hence, the determination of iodide in urine and milk is often required for nutritional, metabolic, and epidemiological studies of thyroid disorder.[10-12]

Various standard techniques such as atomic absorption spectrometry, inductively coupled plasma mass spectrometry, and anodic stripping voltammetry require expensive and sophisticated instrumentation, and/or sample preparation, and are therefore not suitable for real-time and *in situ* analysis. On the other hand, chemosensor based optical determination of cations and anions are a promising strategy given its operational simplicity, high sensitivity with spatial and temporal resolution, and cost. Amongst available colorimetric sensors for Pb^{2+} and I^- ions, their application has been limited given their complex structures, multistep synthetic protocol and the ability to only determine either Pb^{2+} or I^- selectively (Table S1).[5,13-23] Anion sensing mechanisms are primarily based on hydrogen bonding interactions with the NH functionality present in neutral amines, amides, ureas/ thioureas, indoles, pyrroles, guanidinium and imidazolium compounds. To the best of our knowledge, there are few reports of the use of the imine (C=NH) functionality present in a fused heterocyclic compound. Our continuous efforts [24-28] have lead to the development of a novel dual

chemosensor, **PP-1** for the selective and sensitive detection of both Pb^{2+} and I^- ions in aqueous medium.

2. MATERIAL AND METHOD

2.1. Chemicals and instrumentations

All metal salts, reagents and tetra-*n*-butylammonium (TBA) salts of anions were purchased either from S.D. fine chemicals or Sigma Aldrich and were used as received. The metal salts used were $AgClO_4$, $Al(ClO_4)_3.9H_2O$, $Ba(ClO_4)_2$, $Ca(NO_3)_2.4H_2O$, $Cd(ClO_4)_2.H_2O$, $Co(ClO_4)_2.6H_2O$, $Cr(ClO_4)_3.6H_2O$, $Cu(ClO_4)_2.6H_2O$, $Fe(ClO_4)_3.H_2O$, $Fe(ClO_4)_2.xH_2O$, $Hg(NO_3)_2$, LiBr, $Mg(ClO_4)_2$, $Mn(ClO_4)_2.H_2O$, $Ni(ClO_4)_2.6H_2O$, $Pb(ClO_4)_2.3H_2O$ and $Zn(ClO_4)_2.6H_2O$. The TBA salts of anions *viz.*$(n\text{Bu})_4NF.xH_2O$, $(n\text{Bu})_4NCl$, $(n\text{Bu})_4NBr$, $(n\text{Bu})_4NI$, $(n\text{Bu})_4NCN$, $(n\text{Bu})_4NOAc$, $(n\text{Bu})_4NNO_3$, $(n\text{Bu})_4NH_2PO_4$, $(n\text{Bu})_4NClO_4$, $(n\text{Bu})_4NHSO_4$ and $(n\text{Bu})_4NHO.30H_2O$ are used. Spectroscopic grade solvents have been used without further purification. Monitoring of the reactions and purity of the compounds was checked using analytical thin layer chromatography (TLC). Pre-coated silica gel 60 F_{254} (Merck) on alumina plates (7 x 3 cm) were used and visualized in iodine chamber or under a UV lamp.

Melting points were recorded by the open capillary method and are uncorrected. FTIR spectra were recorded on a Perkin-Elmer Spectrum One FTIR spectrometer using KBr pellets and nujol mulls, unless otherwise mentioned. ^1H NMR and ^{13}C NMR were recorded in DMSO-d_6 on a Bruker Avance II 400 NMR spectrometer using TMS as internal standard. UV-Vis spectra were recorded on a U-3900 spectrophotometer (Perkin Elmer Co., USA) using a quartz cuvette having 1 cm path length.

2.2. Synthesis of PP-1[29]

2-Amino-5-bromo-pyridine (0.39 gm, 1 mmol) and KOH (0.25 gm, 2 mmol) were stirred together in 10 mL DMF solution at room temperature for 15-20 min. Then, 2-(bis(methylthio)methylene)malanonitrile (0.5 gm, 1 mmol) was added and the mixture was stirred at room temperature for 3-4 h. The reaction progress was monitored by TLC. After completion of the reaction, excess DMF was removed under reduced pressure, then the residue was subjected to vigorous stirring in ice-water. The aqueous solution was neutralized with 10 % HCl resulting in the formation of yellow precipitate which was collected by filtration. The residue was washed with cold HCl solution (1 %) and dried. The crude product was purified by column chromatography on silica (200-400 mesh) using 10 % ethyl acetate in hexane. Yield: 0.55 gm (81 %); m.p.: 236-238 ^0C; **FTIR [KBr, cm^{-1}]:** 3310, 3092, 3060, 3022, 2205, 1636, 1611, 1541, 1506, 1485, 1360, 1264, 1130, 994, 892, 781. LCMS [ES, m/z (%)]: 297 (97) (M^++2), 295 (100) (M^+). **^1H NMR [DMSO-d_6, 400 MHz, ppm]:** 2.58 (br s, 3H, SCH_3), 7.44-7.46 (d, J=9.3 Hz, 1H, ArH), 7.51 (s, 1H, ArH, -NH), 8.13-8.18 (m, 1H, ArH), 9.30-9.31 (d, J=2.0 Hz, 1H, C=NH, ArH); **^{13}C NMR [DMSO-d_6, 100 MHz, ppm]:** 12.4, 83.6, 110.4, 115.4, 126.6, 128.6, 143.5, 148.6, 167.4; **HRMS (ESI):** ***m/z***: Calculated for $C_{10}H_7BrN_4S$: $[M+H]^+$ 296.17, Found: 296.9670. (%): C, 40.69; H, 2.39 and N, 18.98; found, C, 40.55; H, 2.52 and N, 18.88.

2.3. X-ray Crystallography Data

Single crystal X-ray diffraction data were collected in series of ω-scans using a Stoe IPSD2 image plate diffractometer utilising monochromated Mo radiation (λ = 0.71073 Å). Standard procedures were employed for the integration and processing of the data. Samples were coated in a thin film of perfluoropolyether oil and mounted at the tip of a glass fibre located on a goniometer. Data were collected from crystals held at 150 K in an Oxford Instruments nitrogen gas cryostream.

Crystal structures were solved using routine automatic direct methods implemented within SHELXS-97.[30] Completion of structures was achieved by performing least squares refinement against all unique F^2 values using SHELXL-97. [REF 1] All non-H atoms were refined with anisotropic displacement parameters. Hydrogen atoms were placed using a riding model.

2.4. Spectral studies

Stock solutions of **PP-1** were prepared in acetonitrile (1.0 x 10^{-3} M) and working solutions were prepared by appropriate dilution. The solutions of the cations and anions (1.0 x 10^{-2} M) were prepared in water using the corresponding salts. For the spectroscopic studies, appropriate solutions of **PP-1** and cation/anion were homogeneously mixed into the cuvette to record their spectra.

2.5. Computational studies

Structural optimization of **PP-1** and its host-guest complexes with Pb^{2+} and I^- have been performed by DFT methods in the gas phase using the Gaussian 09W program.[31] All the DFT calculations have been performed using hybrid functional B3LYP (Becke's three parameter hybrid functional using the LYP correlation functional) using basis sets 6-31G (d,p) for the C, H, N, S and Br atoms and LANL2DZ for the Pb and I atoms.

3. RESULTS AND DISCUSSION

The sensor **PP-1** was synthesized as depicted in **Scheme 1**. The structure of **PP-1** was established by various spectroscopic techniques such as FTIR, LCMS, ^1H and ^{13}C-NMR spectroscopy, elemental analysis (Fig. S1, S2, S3, S4 and S5) and also by single crystal X-ray diffraction (Fig. 1‡); the final refinement converged with R1=0.0627. The recognition of cations and anions by **PP-1** was studied using UV- Vis spectroscopy and corroborated via DFT calculations.

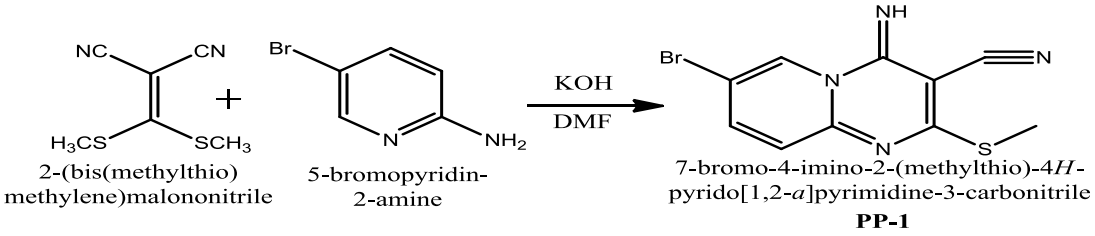

Scheme 1: Synthesis of PP-1.

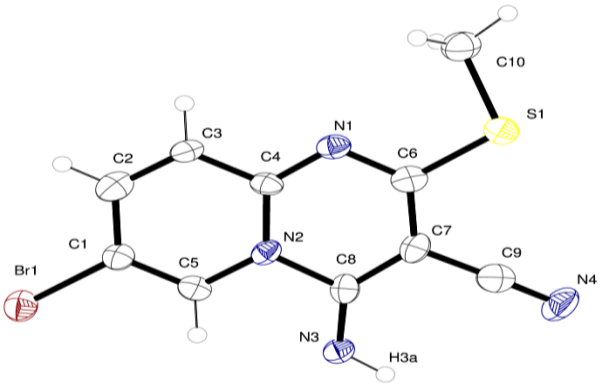

Fig. 1: Single crystal structure of PP-1.

3.1. Studies on the selectivity of PP-1 for Pb^{2+} and I^-

The recognition of **PP-1** (5 x 10^{-5} M, in acetonitrile) towards different cations has been studied by UV-Vis absorption spectroscopy. The absorption spectrum of **PP-1** exhibited a strong peak at 274 nm, a weak band at 319 nm and a broad band in the range 380-435 nm. Upon addition of 2 equivalents of different common cations (Ag^+, Al^{3+}, Ba^{2+}, Cd^{2+}, Co^{2+}, Pb^{2+}, Cr^{3+}, Fe^{2+}, Fe^{3+}, Hg^{2+}, Mg^{2+}, Mn^{2+}, Ni^{2+}, Cu^{2+}, Zn^{2+}; 1 x 10^{-2} M, in water), **PP-1** exhibited remarkable spectral changes in case of Pb^{2+}, Fe^{2+}, Cu^{2+}, Fe^{3+}, Al^{3+} and Cr^{3+} ions with the appearance of a new sharp band at 285 nm. Interestingly, among these selective metal ions, Pb^{2+} exhibited another new peak at 208 nm which allowed for discrimination *versus* Fe^{2+}, Cu^{2+}, Fe^{3+}, Al^{3+} and Cr^{3+} ions (Fig. 2). No significant changes in the absorption spectrum of **PP-1** were observed in the presence of the other tested cations. Thus, this spectral response of **PP-1** permitted the selective recognition of Pb^{2+} in presence of the other fifteen tested cations.

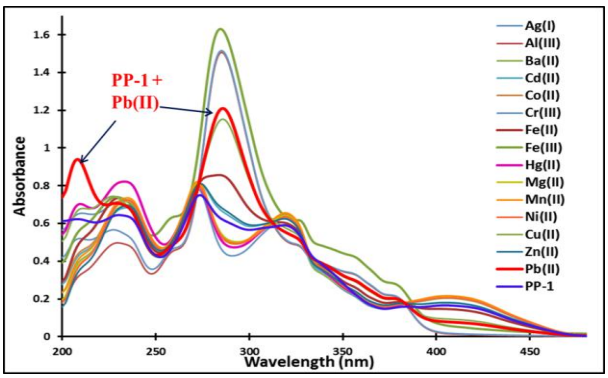

Fig. 2: Changes in the absorption spectra of PP-1 (5 x 10^{-5} M, in CH_3CN) in presence of different tested cations (2 equivalent, 1 x 10^{-2} M, in water).

Meanwhile, the absorption spectrum of **PP-1** (5 x 10^{-5} M, in CH_3CN) exhibited a remarkable change in the presence of iodide ions, whilst the other tested common anions (F^-, AcO^-, Br^-, Cl^-, ClO_4^-, CN^-, $H_2PO_4^-$, HSO_4^-, NO_3^-, OH^-; 1 x 10^{-2} M, in water) had no effect. **PP-1** revealed a new intense band at 240 nm in the presence of iodide (Fig. 3). This observation reflects the I^- recognition capability of **PP-1**.

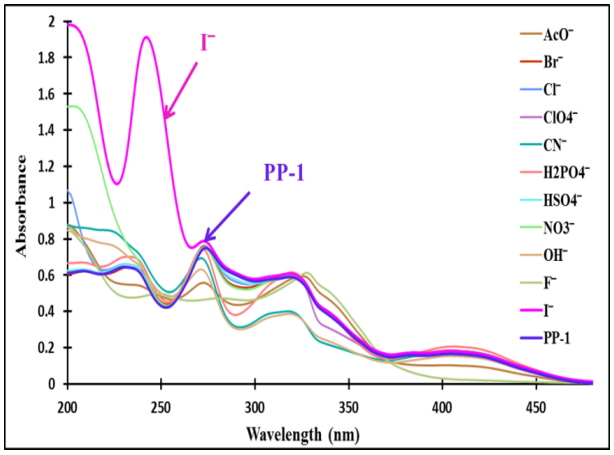

Fig. 3. Changes in the absorption spectra of PP-1 (5 x 10^{-5} M, in CH_3CN) in presence of the tested anions (2 equivalent, 1 x 10^{-2} M, in water).

3.2. Absorption spectroscopic titrations of PP-1 with Pb^{2+} and I^-

To understand the binding interaction, absorption spectroscopic titrations of **PP-1** with Pb^{2+} and I^- ions have been performed. Upon successive addition of Pb^{2+} (0-150 µL, 1 x 10^{-3} M) to **PP-1** (3 mL, 5 x 10^{-5} M, in CH_3CN), the absorption intensities at 208 nm and 285 nm gradually increased, whilst that of 321 nm and 415 nm decreased (Fig. 4). The appearance of isosbestic points at 225 nm, 274 nm, 311 nm and 382 nm clearly supported the presence of an equilibrium interaction between **PP-1** and Pb^{2+} in solution. On the other hand, during the absorption titration of **PP-1** (3 mL, 5 x 10^{-5} M, in CH_3CN) with I^- (0-600 µL, 1 x 10^{-3} M), a remarkable hyperchromic shift at 240 nm and slight hypochromic shifts at 272 nm and 320 nm (Fig. 5) were observed. Additionally, the appearance of an isosbestic point at 266 nm suggested that the two species, namely **PP-1** and its host-guest complex with I^-, existed in equilibrium.

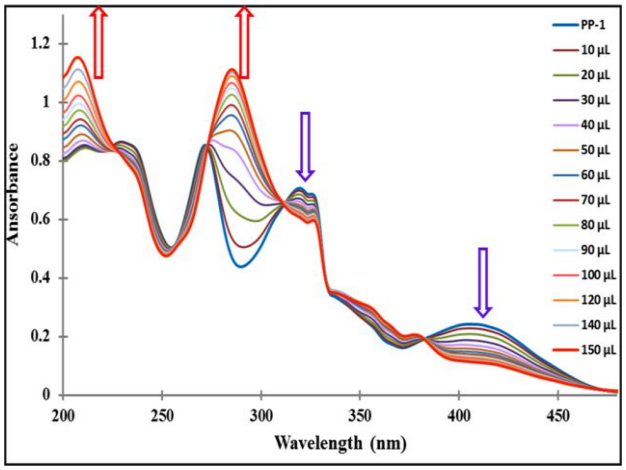

Fig. 4. Changes in the absorption spectra of PP-1 (3 mL, 5 x 10^{-5} M, in CH_3CN) upon gradual addition of Pb^{2+} (0-150 µL, 1 x 10^{-3} M, in water).

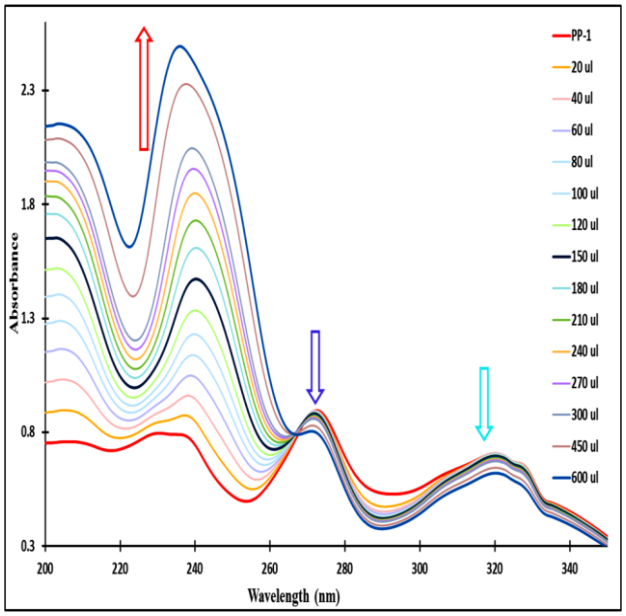

Fig. 5. Changes in the absorption spectra of PP-1 (3 mL, 5 x 10^{-5} M, in CH_3CN) upon gradual addition of I^- (0-600 µL, 1 x 10^{-3} M, in water).

A binding constant of 3.07 x 10^3 M^{-1} for the formation of the [**PP-1**.Pb^{2+}] adduct was calculated from the plot of 1/ΔA *vs.* 1/ [Pb^{2+}] (Fig. 6) using the Benesi-Hildebrand equation.[32] Similarly, the binding constant of **PP-1** for I^- was found to be 1.38 x 10^3 M^{-1} (Fig. 7). The linear Benesi-Hildebrand plot suggested the formation of host-guest adducts between **PP-1** and Pb^{2+}/ I^- ions in a 1:1 mole ratio.

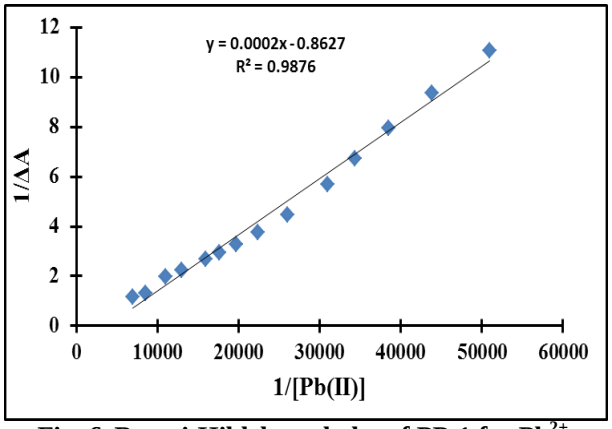

Fig. 6. Benesi-Hildebrand plot of PP-1 for Pb^{2+}.

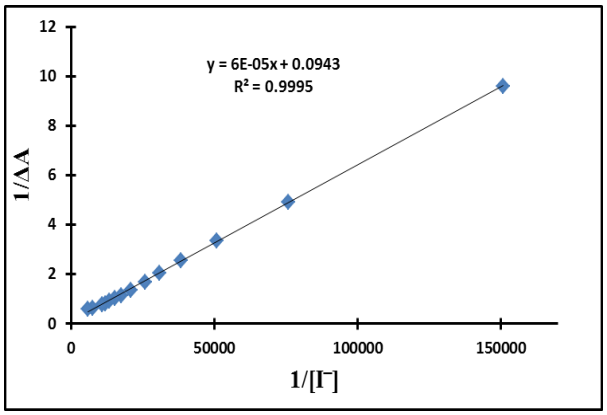

Fig. 7. Benesi-Hildebrand plot of PP-1 for the I^- ion.

The Job's plots also supported the proposed 1:1 binding stoichiometry between **PP-1** and Pb^{2+}/ I^- ions (Fig. S6 and Fig. S7). To confirm the mechanism of binding of Pb^{2+} with **PP-1** we carried out ^{1}H-NMR titration experiments in which the spectra were recorded by adding incremental amounts of lead perchlorate (0, 0.2, 0.5, 1.0 equiv.) to the solution of **PP-1** in DMSO. It was found that the peak corresponding to the =NH proton at □□□ 7.66 ppm shifted slightly to 7.64 with some broadening and finally disappeared on addition of 1.0 equivalents of Pb^{2+} (Fig. S8). This shift and broadening followed by the disappearance of the =NH proton peak suggests the binding of **PP-1** with lead through the nitrogen atom after the abstraction of a proton. More direct evidence for the formation of a 1:1 complex for **PP-1** with Pb^{2+} was obtained from the HR-MS analysis of a mixture of **PP-1** and lead perchlorate in acetonitrile (Fig. S9). A MS peak was observed at 575.2971 which corresponds to [(**PP-1**-H^+).Pb^{2+}.2H_2O+K]. Similarly, we also carried out the ^{1}H NMR spectroscopic titration of **PP-1** in the presence of I^- (Fig. S10). It was found that the peak at □□= 7.66 corresponding to the –NH proton exhibited a slight shift to 7.65 suggesting that hydrogen bonding was involved in the formation of the complex between **PP-1** and I^-. HRMS analysis revealed a peak at 464.9020 corresponding to the species [**PP-1**.I^- .2(H_2O)+Li] (Fig. S11).

3.3. Studies on interference and detection limits

The effect of other common metal ions on the absorption response of **PP-1** towards Pb^{2+} and I^- has been tested *via* competitive experiments. For this purpose, 2 equivalents of the interfering metal ions and 2 equivalents of Pb^{2+} were mixed with **PP-1**, and the absorption spectral changes were plotted (Fig. S12). Similarly, Fig. S13 represents the situation for the I^- ion; no significant interference was observed.

The detection (LOD) and quantification limits (LOQ) of **PP-1** for both Pb^{2+} and I^- have been determined from the respective absorption titration data (Fig. 4 and Fig. 5). To calculate the relative standard deviation, the absorption measurements of ten blank samples were taken. The calibration curves (absorbance *vs* [Pb^{2+}/I^-]) were plotted (Fig. 8 and Fig. 9), and then the obtained slope was used to calculate the LOD and LOQ values. According to the IUPAC definition, the LOD and LOQ was calculated using the standard relationship i.e. LOD = (3.3 x standard deviation)/slope and LOQ = (10 x standard deviation)/slope. The LOD and LOQ for Pb^{2+} were found to be 0.21 µM and 0.64 µM, respectively. The corresponding LOD and LOQ for I^- were 0.10 µM and 0.30 µM, respectively.

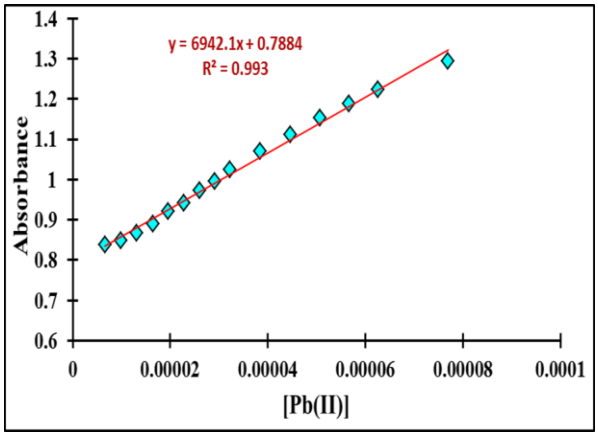

Fig. 8. Linear fitting for the determination of LOD and LOQ of PP-1 for Pb^{2+}.

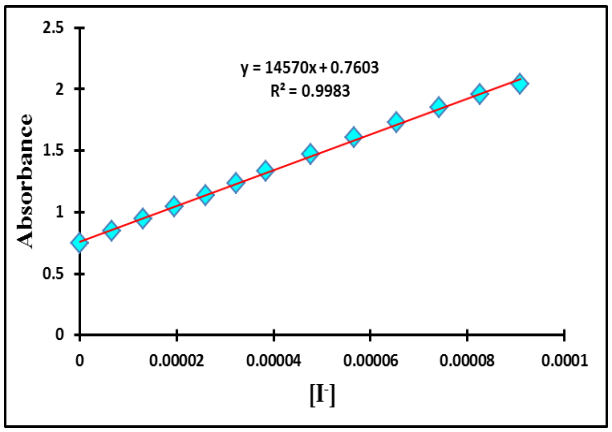

Fig. 9. Linear fitting for the determination of LOD and LOQ of PP-1 for I.

3.4. Computational results

The optimized structures of **PP-1** and its host-guest complexes with Pb^{2+} and I^- were calculated by DFT method at B3LYP/6-31G (d, p)/LANL2DZ level in the gas phase using the Gaussian 09W program [31] and are presented in Fig. 10. The structure of **PP-1** was found to be planar, and the TDDFT calculations generated three peaks at 409, 353 and 330 nm. The optimized structure of **PP-1** is useful to predict the most plausible binding modes for Pb^{2+} and I^-. On complexation with Pb^{2+}, **PP-1** coordinates to Pb^{2+} through the =N atom and the interaction energy [E_{int} = $E_{(ML)}$ - $E_{(L)}$-$E_{(M)}$] was lowered by 185.14 kcal/mol to form a stable complex (Fig. 10b). In contrast, the =NH and Ar-H groups of **PP-1** interact with the iodide ion (Fig. 10c). Further, the analysis of the lowest unoccupied molecular orbital (LUMO) and highest occupied molecular orbital (HOMO) of **PP-1** and its complex with Pb^{2+}/I^- inferred that the electron density in free **PP-1** is uniformly distributed over the entire molecule (**Fig. 10C**). However, the corresponding views of **PP-1**:Pb^{2+}/I^- complexes indicate the intramolecular charge transfer (ICT) occurred between the **PP-1** and Pb^{2+}/I^- with a slight change in the HOMO and LUMO band gap inducing a hyperchromic shift in the absorption spectrum of **PP-1**.

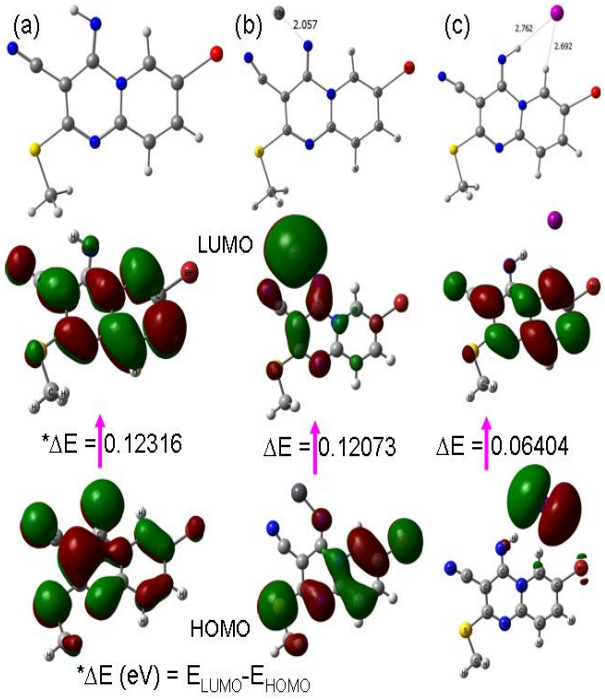

Fig. 10: DFT generated optimized structure and HOMO-LUMO diagrams of (a) PP-1 and adducts with (b) Pb^{2+} and (c) I^-.

4. CONCLUSION

In summary, a novel and easy-to-synthesize pyrido-pyrimidine based dual chemosensor **PP-1** has been developed for the selective detection of Pb^{2+} and I^- ions from 100 % aqueous medium without any interference from other competing ions. The sensor **PP-1** formed host-guest complexes with Pb^{2+} and I^- in a 1:1 binding

stoichiometry with detection limits down to the micromolar range.

5. ACKNOWLEDGEMENT

U. D. Patil is grateful for financial support from Department of Science & Technology, New Delhi, INDIA, (Reg. No. CS-088/2013) & Dr. A.A patil thankful to U.D. Patil for encouragement.

6. Appendix A. Supplementary data

Supplementary data associated with this article can be found online version at doi: 0000000. Journal of Hazardous material.2014...‡ CCDC entry 1020793 contains the supplementary X-ray data for this paper. These data can be obtained free of charge via (please use the link below) by e-mailing data_request@ccdc.cam.ac.uk, or by contacting: The Cambridge Crystallographic Data Centre, 12 Union Road, Cambridge. CB21EZ, UK. Fax: +44(0)1223-336033. This material is available free of charge via the Internet at www.ccdc.cam.ac.uk/data_request/cif.

7. REFERENCES

1. Valeur, B. Leray, I. Design principles of fluorescent molecular sensors for cation recognition, Coord. Chem. Rev., 2000; 205: 3-40.
2. Que, E.L. Domaille, D.W. Chang, C. J. Metals in neurobiology: probing their chemistry and biology with molecular imaging, Chem. Rev., 2008; 108: 1517-1549.
3. Zhang, J.F. Zhou, Y.J. Yoon, Kim, J.S. Recent progress in fluorescent and colorimetric chemosensors for detection of precious metal ions (silver, gold and platinum ions), Chem. Soc. Rev., 2011; 40: 3416-3429.
4. Lu, X.W. Wang, L.J. Lei, K. Huang, J. Zhai, Y.X. Contamination assessment of copper, lead, zinc, manganese and nickel in street dust of Baoji, NW China, J. Hazard. Mater, 2009; 161: 1058-1062.
5. Thakur, A. Mandal, D. Ghosh, S. Sensitive and selective redox, chromogenic, and "turn-on" fluorescent probe for Pb(II) in aqueous environment, Anal. Chem., 2013; 85: 1665-1674.
6. http://www.cdc.gov/nceh/lead/, Center for Disease Control and Prevention 2011.
7. http://www.epa.gov/safewater/mcl.html.
8. Lin-Fu, J.S. Lead poisoning, a century of discovery and rediscovery. In human lead exposure; Needleman, H. L., Ed.; Lewis Publishing: Boca Raton, FL, 1992.
9. Claudio, E.S. Godwin, H.A. Magyar, J.S. Fundamental coordination chemistry, environmental chemistry, and biochemistry of lead(II), Prog. Inorg. Chem., John Wiley & Sons, Inc., 2003; 51: 1-144, and references therein.
10. Haldimann, M. Zimmerli, B. Als, C. Gerber, H. Direct determination of urinary iodine by inductively coupled plasma mass spectrometry using isotope dilution with iodine-129, Clin. Chem., 1998; 44: 817-824, and references therein.
11. Aumont, G. Tressol, J.C. Improved routine method for the determination of total iodine in urine and milk, Analyst, 19863: 841-843.
12. Jalali, F. Rajabi, M.J. Bahrami, Shamsipur, G. M. Preparation of a novel iodide-selective electrode based on iodide-miconazole ion-pair and its application to pharmaceutical analysis, Anal. Sci., 2005; 21: 1533-1535.
13. Baruah, M. Huntimer, E.D. Ahmed, M.S. Hoppe, A.D. Halaweish, F.T. Selective BODIPY based fluorescent chemosensor for imaging Pb^{2+} ion in living cells, Tetrahedron Lett., 2012; 53: 4273-4275.
14. Liu, J. Wu, K. Li, S. Song, T. Han, Y. Li, X. A highly sensitive and selective fluorescent chemosensor for Pb^{2+} ions in an aqueous solution, Dalton Trans, 2013; 42: 3854-3859.
15. Ensafi, A.A. Far, A.K. Meghdadi, S. Highly selective optical-sensing film for lead(II) determination in water samples, J. Hazard. Mater, 2009; 172: 1069-1075.
16. Li, H. Han, C. Zhang, L. Synthesis of cadmium selenide quantum dots modified with thiourea type ligands as fluorescent probes for iodide ions, J. Mater. Chem., 2008; 18: 4543-4548.
17. Ho, H.A. Leclerc, M. New colorimetric and fluorometric chemosensor based on a cationic polythiophene derivative for iodide-specific detection, J. Am. Chem. Soc., 2003; 125: 4412-4413.
18. Hussain, S. De, S. Iyer, P.K. Thiazol-containing conjugated polymer as a visual and fluorometric sensor for iodide and mercury, ACS Appl. Mater. Interfaces, 2013; 5: 2234-2240.
19. Ghosh, K. Kar, D. Fluorometric recognition of both dihydrogen phosphate and iodide by a new flexible anthracene linked benzimidazolium-based receptor, Beilstein J. Org. Chem., 2011; 7: 254-264.
20. Jua, H. Lee, M.H. Kim, J. Kim, J.S. Kim, J. Rhodamine-based chemosensing monolayers on glass as a facile fluorescent "turn-on" sensing film for selective detection of Pb^{2+}, Talanta, 2011; 83: 1359-1363.
21. Yang, J. Zhou, C. Liu, C. Li, Liu, Y. H. Li, Y. Zhu, D. A dual sensor of fluorescent and colorimetric for the rapid detection of lead, Analyst, 2012; 137: 1446-1450.
22. Maa, L. Li, H. Wu, Y. A pyrene-containing fluorescent sensor with high selectivity for lead (II) ion in water with dual illustration of ground-state dimer, Sens. Actuators B, 2009; 143: 25-29.
23. Park, J. Kim, Y. A colorimetric probe for the selective naked-eye detection of Pb(II) ions in aqueous media, Analyst, 2012; 137: 3246-3248.
24. Chandel, M. Roy, S.M. Sharma, D. Sahoo, S.K. Patel, A. Kumari, P. Dhale, R.S. Ashok, K.S.K. Nandre, J.P. Patil, U.D. Anion recognition ability of a novel azo dye derived from 4-hydroxycoumarin, J. Luminesc, 2014; 154: 515-519.
25. Kuwar, A.S. Fegade, U.A. Tayade, K.C. Patil, U.D. Puschmann, H. Gite, V.V. Dalal, D.S. Bendre, R.S.

Bis(2-hydroxy-3-isopropyl-6-methyl-benzaldehyde)ethylenediamine: a novel cation sensor, J. Fluoresc, 2013; 23: 859-864.
26. Nandre, J. Patil, S. Patil, V. Yu, F. Chen, L. Sahoo, S. Prior, T. Redshaw, C. Mahulikar, P. Patil, U. A novel fluorescent "turn-on" chemosensor for nanomolar detection of Fe(III) from aqueous solution and its application in living cells imaging, Biosens. Bioelectron, 2014; 61: 612-617.
27. Patil, S.R. Nandre, J.P. Jadhav, D. Bothra, S. Sahoo, S.K. Devi, M. Pradeep, C.P. Mahulikar, P.P. Patil, U.D. Imatinib intermediate as a two in one dual channel sensor for the recognition of Cu^{2+} and I^{-} ions in aqueous media and its practical applications, Dalton Trans, 2014; 43: 13299-13306.
28. Nandre, J. Patil, S. Patil, P. Sahoo, S. Redshaw, C. Mahulikar, P. Patil, U. The amidine based colorimetric sensor for Fe^{3+}, Fe^{2+}, and Cu^{2+} in aqueous medium, J. Fluoresc, 2014. DOI: 10.1007/s10895-014-1438-4.
29. Indian J. Chem., Sect B, 2004; 43: 1561-1564.
30. Sheldrick, G. Acta Crystallogr. Sect. A: Found. Crystallogr, 2008, 64: 112-122.
31. Schlegel, H.B. Scuseria, G.E. Robb, M.A. Cheeseman, J.R. G. V. Barone, B. Mennucci, G.A. Petersson, H. Nakatsuji, M. Caricato, Li, X. Hratchian, H.P. Izmaylov, A.F. Bloino, Zheng, J. G. Sonnenberg, J. Hada, L. Ehara, M. M. K. Toyota, R. Fukuda, J. Hasegawa, M. Ishida, T. Nakajima, Y. Honda, O. Kitao, H. Nakai, T. Vreven, J.A. Montgomery, Jr., Peralta, J.E. Ogliaro, F. Bearpark, M. Heyd, J.J. Brothers, E. Kudin, K.N. Staroverov, V.N. Kobayashi, R. Normand, J. Raghavachari, K. Rendell, A. Burant, J.C. Iyengar, S.S. Tomasi, J. Cossi, M. Rega, N. Millam, J.M. Klene M., Knox, J.E. Cross, J.B. Bakken, V. Adamo, C. Jaramillo, J. Gomperts, R. Stratmann, R.E. Yazyev, O. Austin, A.J. Cammi, R. Pomelli, C. Ochterski, J.W. Martin, R.L. Morokuma, K. Zakrzewski, V.G. Voth, G.A. Salvador, P. Dannenberg, J.J. Dapprich, S. Daniels, A.D. Farkas, Ö. Foresman, J.B. Ortiz, J.V. Cioslowski, J. Fox, D.J. Gaussian 09, Revision A.1, Gaussian, Inc., Wallingford CT, 2009.
32. Benesi, H.A. Hildebrand, J.H. A spectrophotometric investigation of the interaction of iodine with aromatic hydrocarbons, J. Am. Chem. Soc., 1949; 71: 2703-2707.